Supplementary materials for:

Three distinct Holocene intervals revealed in NW Madagascar: evidence from two stalagmites from two caves, and implications for ITCZ dynamics

Voarintsoa, Ny Riavo G.[1*], L. Bruce Railsback[1], George A. Brook[2], Lixin Wang[2], Gayatri Kathayat[3], Hai Cheng[3,4], Xianglei Li[3], R. Lawrence Edwards[4], Rakotondrazafy Amos Fety Michel[5], Madison Razanatseheno Marie Olga[5]

[1] Department of Geology, University of Georgia, Athens, GA 30602-2501 U.S.A.
[2] Department of Geography, University of Georgia, Athens, Georgia, 30602-2502 U.S.A.
[3] Institute of Global Environmental Change, Xi'an Jiaotong University, Xi'an, Shaanxi 710049, P.R. China
[4] Department of Earth Sciences, University of Minnesota, Minneapolis, Minnesota 55455, U.S.A.
[5] Department of Geology, University of Antananarivo, Madagascar

*Correspondence to: Ny Riavo Voarintsoa (nv1@uga.edu or nyriavony@gmail.com)

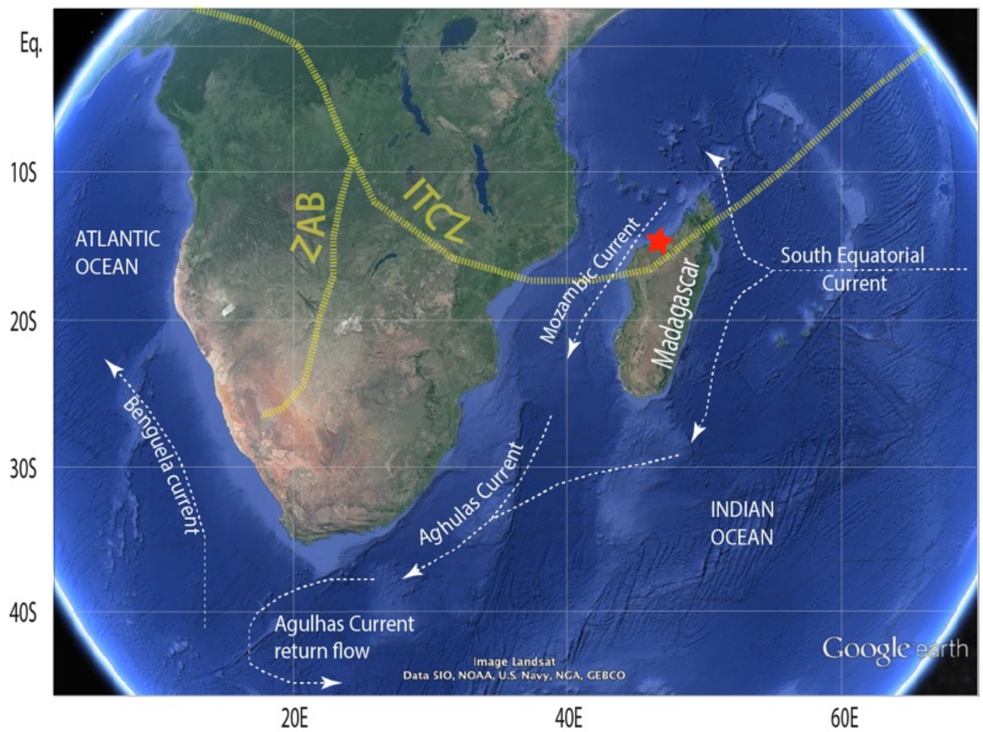

Figure S1: **Google Earth image putting Madagascar into perspective** with regard to oceanic currents and convergence zones (ITCZ and ZAB, Zaire Aire Boundary). The map of the currents was obtained from Lindesay, 1998 and Schott and McCreary (2001). The map of the ITCZ and ZAB was adopted from Gasse (2000). The red star indicates the study location.

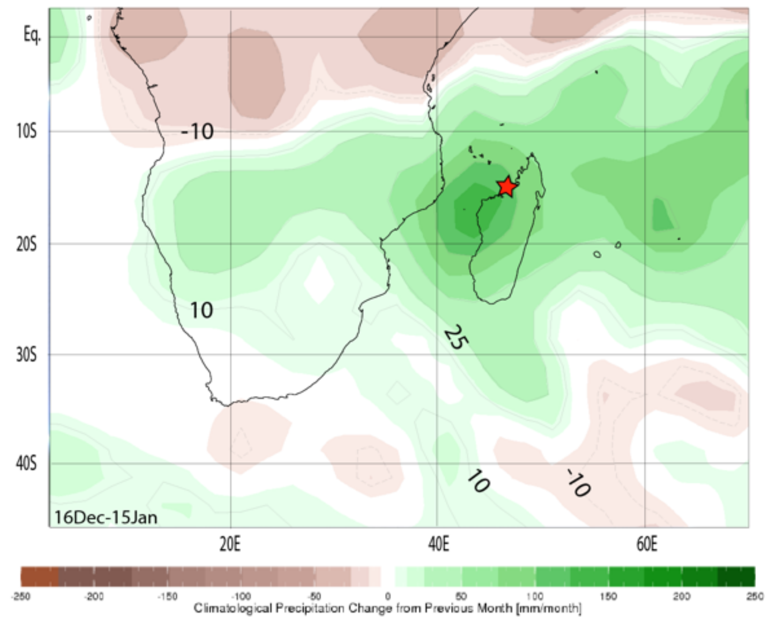

Figure S2: **Climate setting**. Map of summer precipitation between December 16 and January 15 (the wettest months) in Madagascar. Red star indicates the study area. Source: http://iridl.ldeo.columbia.edu/ (accessed August 31, 2016)

Figure S3: **Cave locations**. Google Earth image showing the location of the two caves Anjohibe (ANJB) and Anjokipoty (ANJK) Caves and the current extent of vegetation cover in northwestern Madagascar.

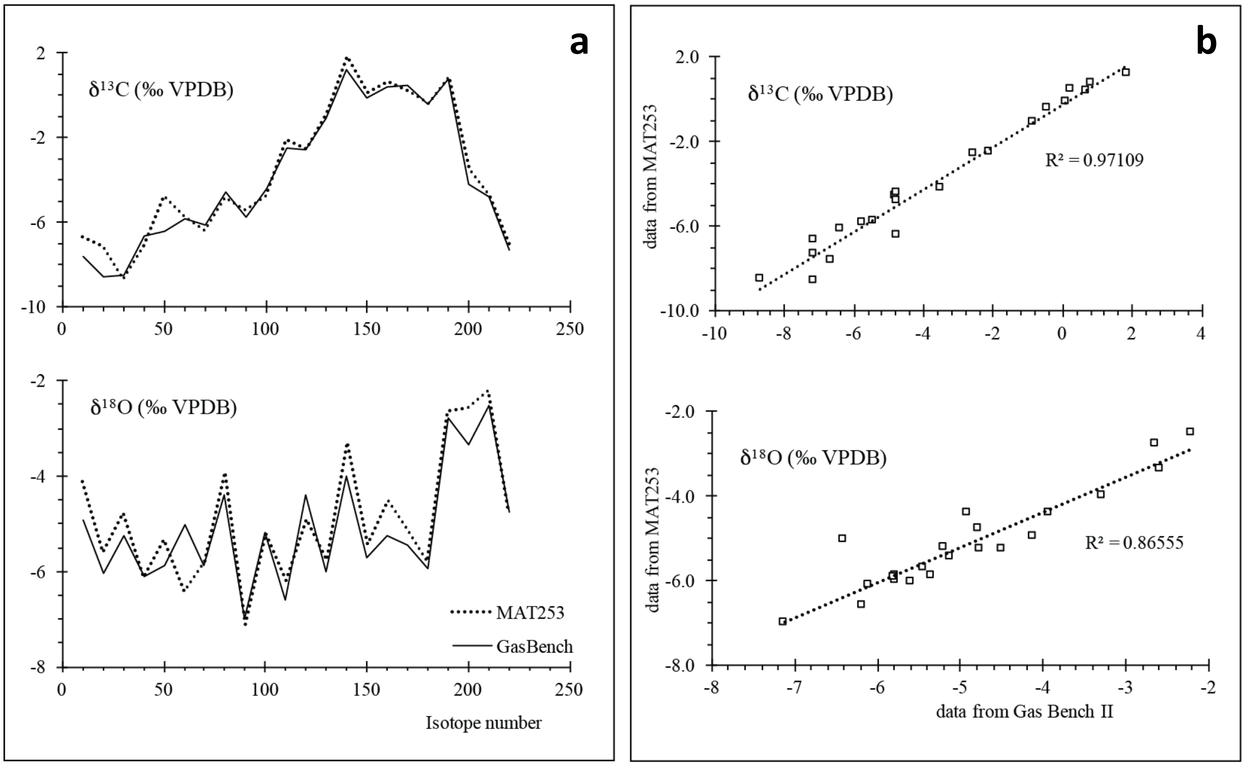

Figure S4: Comparison between MAT 253 and Gas Bench II stable isotope results on Stalagmite MAJ-5, showing similarity in the results. a) Depth series of $\delta^{13}C$ and $\delta^{18}O$. b) Scatterplots of $\delta^{13}C$ and $\delta^{18}O$.

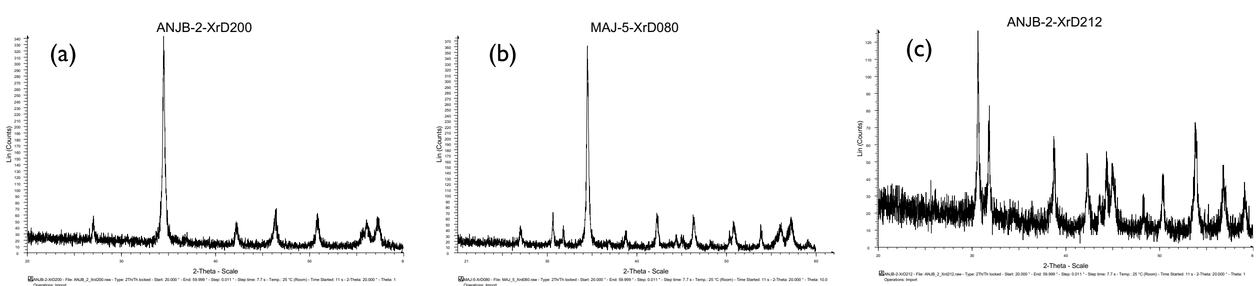

Figure S5: Selected X-ray diffraction spectra of the three types of mineralogy identified in Stalagmite ANJB-2 and MAJ-5. (a) 100% calcite. (b) 50% calcite-50% aragonite. (c) 100% aragonite.

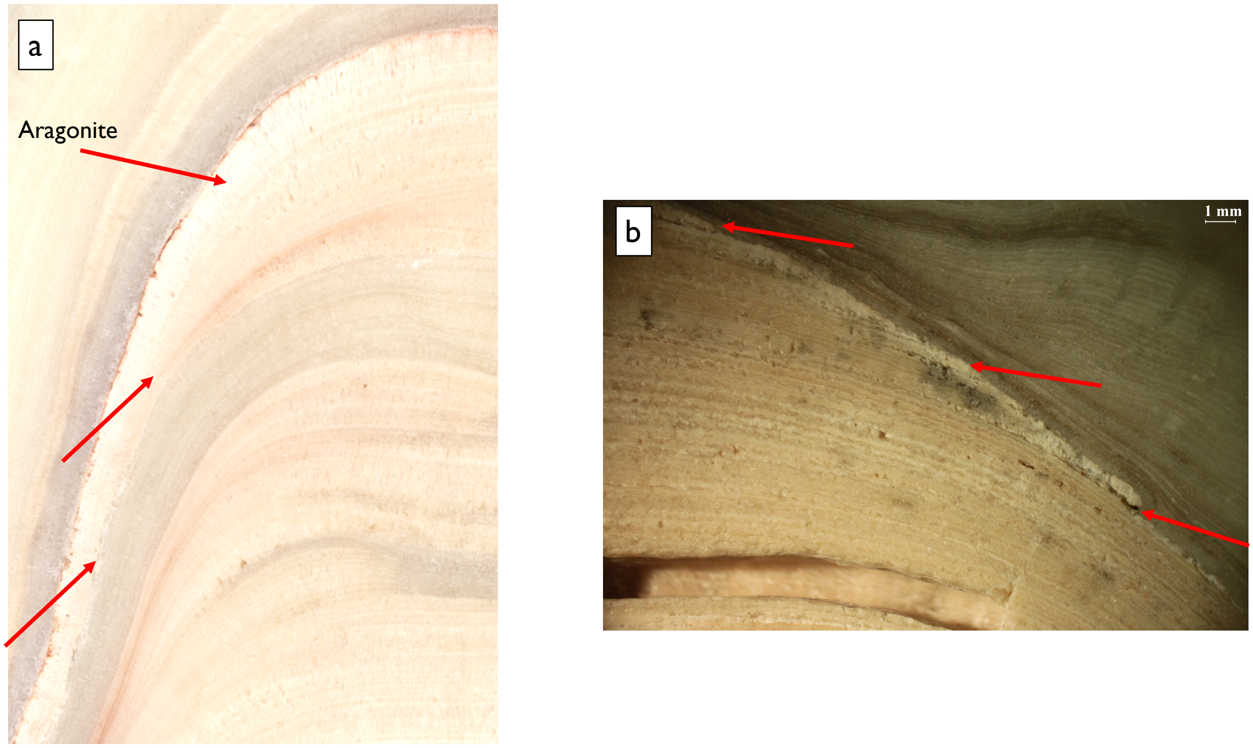

Figure S6: **Photographs illustrating the mid-Holocene hiatus**. Photographs showing the Type L layer-bounding surfaces in Stalagmite ANJB-2 (a) and in Stalagmite MAJ-5 (b). Pinching of layers toward the flank are indicated with arrows. Also, note the white and porous layer of aragonite in Stalagmite ANB-2 that is capped with a very thin brown layer.

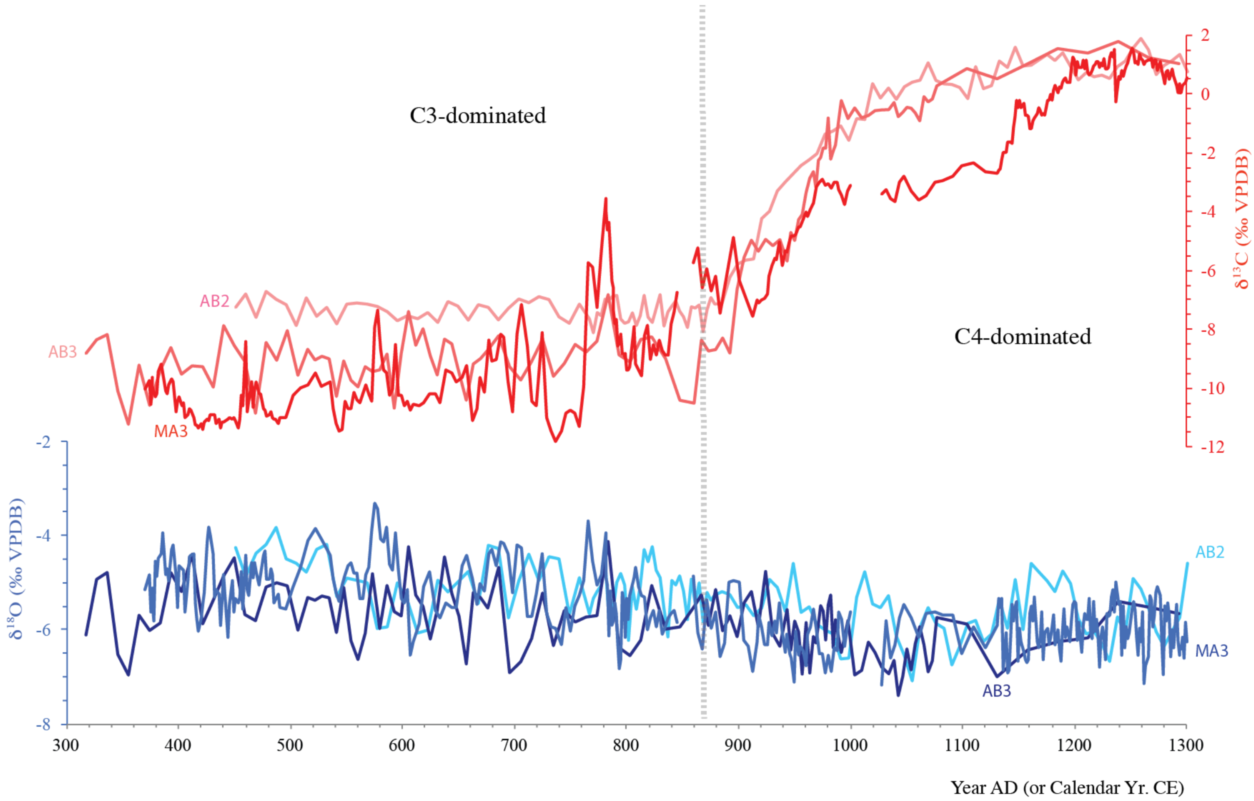

Figure S7: **Stable isotope profile** of $\delta^{18}O$ and $\delta^{13}C$ of the late Holocene in Madagascar from Anjohibe Cave's stalagmites showing the $\delta^{13}C$ from C_3-dominated to C_4-dominated vegetation (Burns et al., 2016; Voarintsoa et al., in revision). Note that the age scale is in year AD.

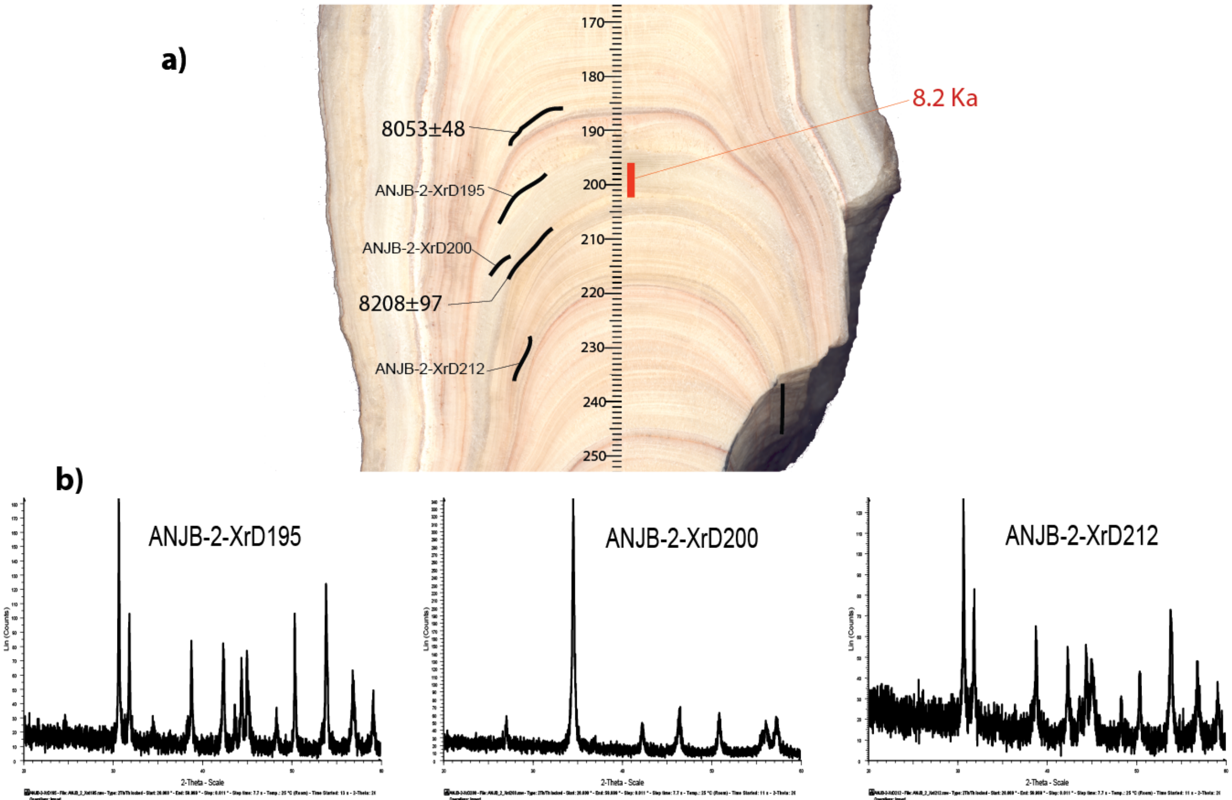

Figure S8: **The 8.2 ka event identified in Stalagmite ANJB-2**. a) Scanned image of a portion of Stalagmite ANJB-2 showing the 8.2 ka event and the corresponding trenches for radiometric dating and X-ray diffraction analyses. b) X-ray diffraction spectra of the stalagmite layers at 195, 200, and 212 mm from the top of the stalagmite.

Supplementary text 1: Possible climatic response of the latitudinal migration of the ITCZ

The ITCZ migrates southward in austral summer and northward in boreal summer in response to seasonal insolation. Climate simulations have also reported long-term migration of the ITCZ, the causes of which have been ascribed to changes in insolation and difference in temperature between the Northern and the Southern Hemisphere (e.g. Chiang and Bitz, 2005; Broccolli et al., 2006; Braconnot et al., 2007). The climatic responses to the ITCZ dynamics can vary from region to region and from one time interval to another. Here, we attempt to provide different conceptualized models to understand the climatic regime in Madagascar during the early, the middle, and the late Holocene (as proposed in Sect. 5.2. of the manuscript).

Dry conditions in Madagascar could be conceptualized as dry years, such as modeled in case 1 (Fig. S9). In that model, austral summer months receive less rainfall and austral winter months could receive no rainfall. This model could be used to conceptualize the climatic response in Madagascar when the ITCZ moves north, such as during the mid-Holocene.

Wet conditions in Madagascar could be conceptualized as wet years, such as modeled in case 2 and case 3 (Fig. S9). Case 2 suggests that austral summer months receive rain as well as austral winter months, thus it suggests less seasonality. Although the amount of rainfall received during winter months cannot be easily estimated, this model could be used to understand the climatic response in Madagascar during the early Holocene when the southern hemisphere winter insolation was relatively greater than the northen Hemisphere winter insolation (Fig. 5a). The ITCZ was already moved southward due to the globally cold conditions (Figs. 6a, c), and because of the higher winter insolation in the SH, heating of land would bring additional precipitation during austral winter. Case 3 suggests that austral summers receive more rainfall than normal years, but austral winters stay dry or with little precipitation, thus seasonality must have been stronger. This scenario could be used to understand the climatic response in Madagascar during the late Holocene when the southern hemisphere summer insolation was greater than the northern hemisphere summer insolation (Fig. 5a). Globally cooler conditions (Figs. 6a, b) already suggest a southward migration of the ITCZ, and the greater SH summer insolation could have intensified the monsoonal rainfall in northwestern Madagascar during austral summers.

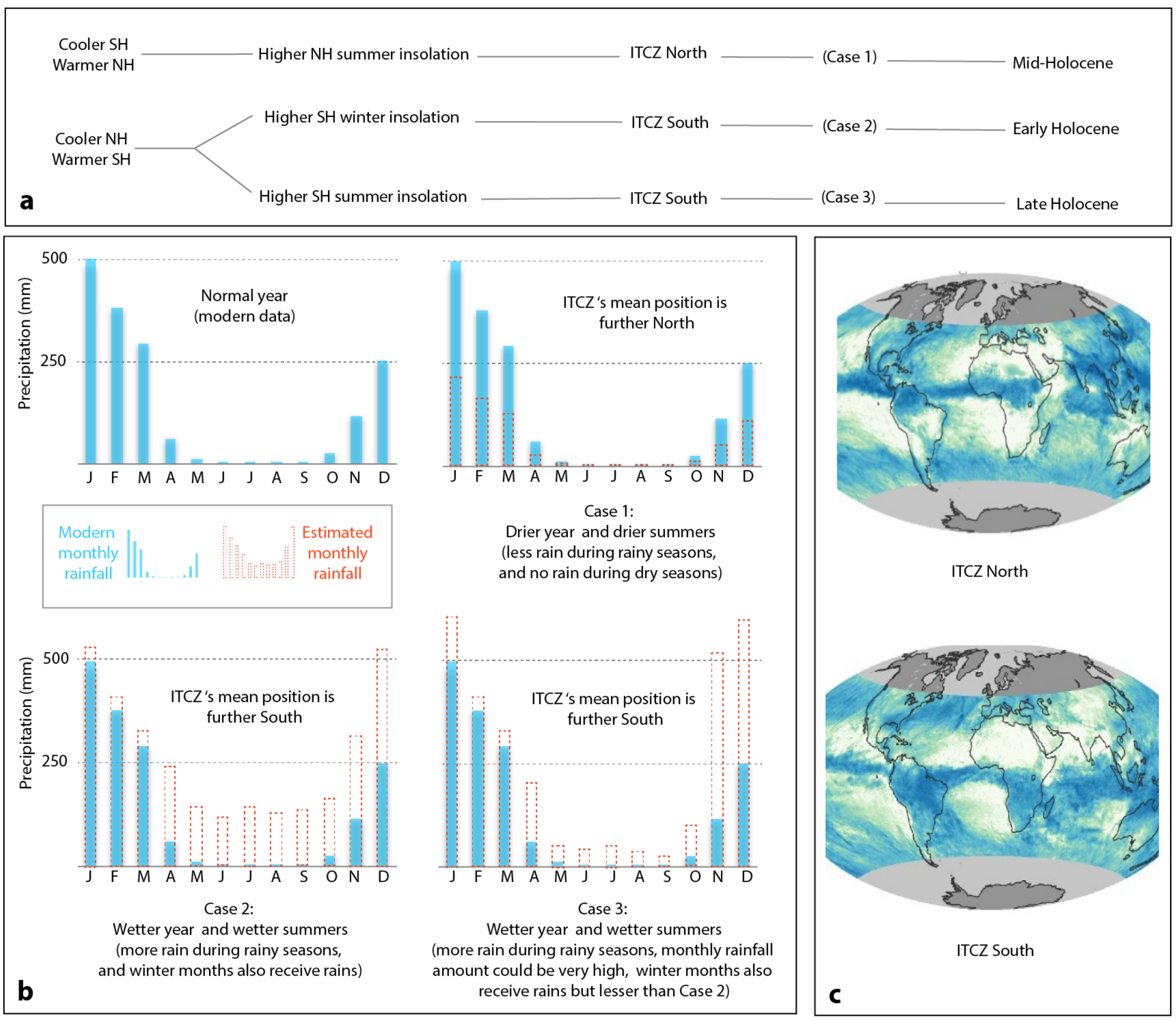

Figure S9: **Conceptualizing the different possible outcomes of the long-term latitudinal migration of the ITCZ**. a) Highlighting the three possible scenarios of the Holocene. b) Barplots of monthly rainfall in northwestern Madagascar, using the modern data as a reference to estimating the region's paleoclimate during drier and wetter conditions. c) Global rainfall maps from NASA (same source as Fig. 1 in the manuscript). These maps are modern, but they are only shown here to give a better perspective of the position of Madagascar when the ITCZ is relatively north or south.

Tables

Table S1: ^{230}Th dating results for Stalagmite ANJB-2. The error is 2 σ error. Dft= distance from the top of the stalagmite.

Dft (mm)	Sample no.	^{238}U (ppb)	^{232}Th (ppt)	^{230}Th / ^{232}Th (atomic x10^{-6})	d^{234}U* (measured)	^{230}Th / ^{238}U (activity)	^{230}Th Age (yr) (uncorrected)	^{230}Th Age (yr) (corrected)	d^{234}U$_{Initial}$** (corrected)	^{230}Th Age (yr BP)*** (corrected)
3	ANJ-B-2-U003	3371 ±11	39850 ±809	10 ±0	5.2 ±2.0	0.0070 ±0.0001	761 ±7	419 ±243	5 ±2	355 ±243
8	ANJB-2-008	194.6 ±0.3	410 ±8	20 ±3	3.6 ±1.7	0.0026 ±0.0004	284 ±47	223 ±64	4 ±2	161 ±64
25	ANJB-2-025	4646.6 ±6.6	1594 ±32	216 ±5	3.4 ±1.4	0.0045 ±0.0001	489 ±7	479 ±10	3 ±1	417 ±10
47	ANJ-B-2-U047	64 ±0	634 ±15	31 ±12	3.0 ±4.3	0.0187 ±0.0074	2052 ±822	1762 ±845	3 ±4	1697 ±845
53	ANJ-B-2-U053R	134 ±0	2325 ±47	20 ±4	4.6 ±2.0	0.0211 ±0.0037	2313 ±416	1808 ±547	5 ±2	1743 ±547
72	ANJB-2-072	67.8 ±0.1	382 ±8	48 ±3	8.5 ±2.4	0.0163 ±0.0008	1778 ±93	1615 ±147	9 ±2	1553 ±147
92	ANJ-B-2-U092	78 ±0	180 ±8	92 ±40	5.1 ±3.5	0.0129 ±0.0056	1408 ±610	1341 ±612	5 ±4	1276 ±612
105	ANJ-B-2-U105	117 ±0	229 ±9	113 ±34	13.5 ±2.9	0.0134 ±0.0040	1450 ±432	1393 ±434	14 ±3	1329 ±434
112	ANJ-B-2-U112	1322 ±2	7456 ±150	42 ±2	8.5 ±2.0	0.0145 ±0.0005	1576 ±50	1413 ±125	9 ±2	1348 ±125
116	AB-1a	130.9 ±0.2	530 ±14	136.7 ±16.7	27.0 ±3.0	0.033539275 ±0.00400	3620 ±439	3506 ±446	27.2 ±3.0	3444 ±446
118	AB-2a	2569.8 ±2.9	5266 ±106	580.4 ±11.9	7.5 ±1.6	0.072126026 ±0.00032	8100 ±40	8040 ±58	7.6 ±1.6	7978 ±58
120	ANJ-B-2-U120	1710 ±4	20753 ±418	108 ±2	9.1 ±2.3	0.0796 ±0.0004	8955 ±48	8605 ±252	9 ±2	8541 ±252
120	ANJ-B-2-U120R	2075 ±3	13340 ±268	197 ±4	6.3 ±1.5	0.0767 ±0.0003	8640 ±38	8454 ±137	6 ±2	8389 ±137
130	ANJB-2-130	3042.4 ±3.8	7448 ±149	477 ±10	6.2 ±1.5	0.0709 ±0.0002	7966 ±26	7895 ±57	6 ±2	7833 ±57
160	ANJB-2-160	2994.8 ±4.1	2484 ±50	1416 ±29	4.3 ±1.5	0.0712 ±0.0002	8021 ±30	7997 ±35	4 ±2	7935 ±35
185	ANJ-B-2-U185	3490 ±5	6040 ±122	690 ±14	3.6 ±1.7	0.0724 ±0.0003	8167 ±33	8117 ±48	4 ±2	8053 ±48
201	ANJ-B-2-U205	574 ±1	1881 ±38	374 ±8	5.7 ±1.8	0.0743 ±0.0006	8367 ±70	8272 ±97	6 ±2	8208 ±97
215	ANJ-B-2-U215	3146 ±4	5418 ±109	713 ±15	7.0 ±1.5	0.0745 ±0.0003	8379 ±33	8329 ±48	7 ±2	8265 ±48
251	ANJ-B-2-U251	4246 ±5	7290 ±147	745 ±15	6.3 ±1.3	0.0776 ±0.0002	8750 ±27	8700 ±44	6 ±1	8636 ±44
275	ANJ-B-2-U275	6077 ±9	9132 ±184	861 ±17	4.5 ±1.5	0.0785 ±0.0002	8867 ±32	8823 ±44	5 ±2	8759 ±44
280	MAJ-B-2-U280	5721 ±18	5408 ±110	1360 ±28	2.4 ±1.6	0.0780 ±0.0003	8828 ±36	8801 ±41	2 ±2	8737 ±41
302	ANJ-B-2-U302	9833 ±44	1617 ±33	8024 ±166	5.2 ±1.9	0.0800 ±0.0004	9045 ±50	9041 ±50	5 ±2	8977 ±50

U decay constants: $\lambda_{238} = 1.55125\text{x}10^{-10}$ (Jaffey et al., 1971) and $\lambda_{234} = 2.82206\text{x}10^{-6}$ (Cheng et al., 2013). Th decay constant: $\lambda_{230} = 9.1705\text{x}10^{-6}$ (Cheng et al., 2013).

*$\delta^{234}U = ([^{234}U/^{238}U]_{activity} - 1)\text{x}1000$. ** $\delta^{234}U_{initial}$ was calculated based on ^{230}Th age (T), i.e., $\delta^{234}U_{initial} = \delta^{234}U_{measured} \text{ x } e\lambda^{234\text{x}T}$.

Corrected ^{230}Th ages assume the initial $^{230}Th/^{232}Th$ atomic ratio of $4.4 \pm 2.2 \text{ x}10^{-6}$. Those are the values for a material at secular equilibrium, with the bulk earth $^{232}Th/^{238}U$ value of 3.8. The errors are arbitrarily assumed to be 50%.

***B.P. stands for “Before Present” where the “Present” is defined as the year 1950 A.D.

Table S2: ^{230}Th dating results for Stalagmite MAJ-5. The error is 2 σ error. Dft= distance from the top of the stalagmite.

Dft (mm)	Sample no.	^{238}U (ppb)		^{232}Th (ppt)		$^{230}Th / ^{232}Th$ (atomic x10^{-6})		$d^{234}U$* (measured)		$^{230}Th / ^{238}U$ (activity)		^{230}Th Age (yr) (uncorrected)		^{230}Th Age (yr) (corrected)		$d^{234}U_{Initial}$** (corrected)		^{230}Th Age (yr BP)*** (corrected)	
1	MAJ-5-U001	2734	±15	3044	±63	33	±1	-3.2	±2.7	0.0023	±0.0000	246	±5	214	±24	-3	±3	150	±24
10	MAJ-5-U010	6691	±38	22757	±474	27	±1	-3.1	±3.6	0.0056	±0.0001	609	±7	510	±71	-3	±4	446	±71
22	MAJ-5-U022	3292	±4	11633	±234	31	±1	-3.0	±1.5	0.0067	±0.0001	736	±14	633	±74	-3	±1	569	±74
41	MAJ-5-U041	1380	±3	10604	±213	32	±1	-1.1	±2.1	0.0147	±0.0001	1617	±15	1393	±159	-1	±2	1329	±159
50	MAJ-5-U050	1224	±4	4144	±84	40	±1	-2.9	±2.4	0.0082	±0.0001	898	±15	799	±71	-3	±2	735	±71
60	MAJ-5-U060	1578	±3	14591	±293	31	±1	-0.9	±2.6	0.0173	±0.0005	1901	±56	1631	±199	-1	±3	1567	±199
66	MAJ-5-U066	12609	±83	38990	±842	461	±10	-4.6	±2.9	0.0865	±0.0006	9912	±81	9821	±103	-5	±3	9757	±103
80	MAJ-5-U080	11684	±16	27838	±559	598	±12	-2.6	±1.2	0.0864	±0.0002	9882	±24	9813	±55	-3	±1	9749	±55
89	MAJ-5-U089	10930	±12	30247	±606	519	±10	-1.2	±1.3	0.0870	±0.0002	9941	±29	9860	±64	-1	±1	9796	±64

U decay constants: $\lambda_{238} = 1.55125\text{x}10^{-10}$ (Jaffey et al., 1971) and $\lambda_{234} = 2.82206\text{x}10^{-6}$ (Cheng et al., 2013). Th decay constant: $\lambda_{230} = 9.1705\text{x}10^{-6}$ (Cheng et al., 2013).

*$\delta^{234}U = ([^{234}U/^{238}U]_{activity} - 1)\text{x}1000$. ** $\delta^{234}U_{initial}$ was calculated based on ^{230}Th age (T), i.e., $\delta^{234}U_{initial} = \delta^{234}U_{measured} \text{ x } e\lambda^{234\text{x}T}$.

Corrected ^{230}Th ages assume the initial $^{230}Th/^{232}Th$ atomic ratio of $4.4 \pm 2.2 \text{ x}10^{-6}$. Those are the values for a material at secular equilibrium, with the bulk earth $^{232}Th/^{238}U$ value of 3.8. The errors are arbitrarily assumed to be 50%.

***B.P. stands for “Before Present” where the “Present” is defined as the year 1950 A.D.

References

Braconnot, P., Otto-Bliesner, B., Harrison, S., Joussaume, S., Peterchmitt, J. Y., Abe-Ouchi, A., Crucifix, M., Driesschaert, E., Fichefet, T., Hewitt, C. D., Kageyama, M., Kitoh, A., Laine, A., Loutre, M. F., Marti, O., Merkel, U., Ramstein, G., Valdes, P., Weber, S. L., Yu, Y., and Zhao, Y.: Results of PMIP2 coupled simulations of the Mid-Holocene and Last Glacial Maximum - Part 1: experiments and large-scale features, Clim Past, 3, 261-277, 2007.

Broccoli, A. J., Dahl, K. A., and Stouffer, R. J.: Response of the ITCZ to Northern Hemisphere cooling, Geophys Res Lett, 33, 10.1029/2005gl024546, 2006.

Burns, S. J., Godfrey, L. R., Faina, P., McGee, D., Hardt, B., Ranivoharimanana, L., and Randrianasy, J.: Rapid human-induced landscape transformation in Madagascar at the end of the first millennium of the Common Era, Quaternary Sci Rev, 134, 92-99, 10.1016/j.quascirev.2016.01.007, 2016.

Cheng, H., Edwards, R. L., Shen, C. C., Polyak, V. J., Asmerom, Y., Woodhead, J., Hellstrom, J., Wang, Y. J., Kong, X. G., Spotl, C., Wang, X. F., and Alexander, E. C.: Improvements in Th-230 dating, Th-230 and U-234 half-life values, and U-Th isotopic measurements by multi-collector inductively coupled plasma mass spectrometry, Earth Planet Sc Lett, 371, 82-91, Doi 10.1016/J.Epsl.2013.04.006, 2013.

Chiang, J. C. H., and Bitz, C. M.: Influence of high latitude ice cover on the marine Intertropical Convergence Zone, Clim Dynam, 25, 477-496, 10.1007/s00382-005-0040-5, 2005.

Gasse, F.: Hydrological changes in the African tropics since the Last Glacial Maximum, Quaternary Sci Rev, 19, 189-211, Doi 10.1016/S0277-3791(99)00061-X, 2000.

Jaffey, A. H., Flynn, K. F., Glendenin, L. E., Bentley, W. C., and Essling, A. M.: Precision measurement of half-lives and specific activities of U-235 and U-238, Phys Rev C, 4, 1889-1906, DOI 10.1103/PhysRevC.4.1889, 1971.

Lindesay, J. A.: Present Climates of Southern Africa, in: Climates of the Southern Continents: Present, Past and Future, edited by: Hobbs, J. E., Lindesay, J. A., and Bridgman, H. A., John Wiley & Sons Ltd., England, 5-62, 1998.

Schott, F. A., and McCreary, J. P.: The monsoon circulation of the Indian Ocean, Prog Oceanogr, 51, 1-123, Doi 10.1016/S0079-6611(01)00083-0, 2001.

Voarintsoa, N.R. G., Wang, L., Railsback, L.B., Brook, G.A., Liang, F., Cheng, H., Edwards, R.L.: Multiple proxy analyses of a U/Th-dated stalagmite to reconstruct paleoenvironmental changes in northwestern Madagascar between AD 370 and AD 1300, Palaeogeography, Palaeoclimatology, Palaeoecology, under review.